Heliyon 5 (2019) e02471

Contents lists available at ScienceDirect

Heliyon

journal homepage: www.heliyon.com

Research article

Influence of trace additions of titanium on grain characteristics, conductivity and mechanical properties of copper-silicon-titanium alloys

Kingsley C. Nnakwo [a,*], Christopher N. Mbah [b], Eugene E. Nnuka [a]

[a] Department of Metallurgical and Materials Engineering, Nnamdi Azikiwe University, Awka, Nigeria
[b] Department of Metallurgical and Materials Engineering, Enugu State University of Science and Technology, Agbani, Nigeria

ARTICLE INFO

Keywords:
Computer science
Physics
Materials science
Chemistry
Copper
Titanium
Grain size
Grain morphology
Silicon
Conductivity

ABSTRACT

The main objective of this research is to explore the influence of trace additions of titanium on grain characteristics (morphology and size), conductivity, and mechanical properties of copper-silicon-titanium alloys. The alloys compositions were designed using response surface optimal design (RSOD). The designed alloy compositions were melted, cast, and subjected to normalizing heat treatment at 900 °C for 0.5 hr. The grain characteristics and the elemental constituents of the produced alloys were analyzed using an optical microscope (OM), scanning electron microscopy (SEM), and x-ray fluorescence spectroscopy. The average grain size and distribution were also determined. The properties investigated were percentage elongation, tensile strength, hardness, electrical conductivity, and density. The results were analyzed statistically using analysis of variance (ANOVA) to obtain the significance of titanium content on the tested properties and to generate statistical model equations for future applications. The experimental results were optimized to ascertain the optimal alloy composition and properties. The OM and SEM results revealed a decrease in the average grain size of the parent alloy (Cu–3Si) from ≈10.1 μm to ≈4.4 μm and change in grain morphology after adding titanium, leading to improvement of properties. The results were confirmed to be statistically significant. The optimization results revealed Cu–3Si-0.47wt%Ti as the optimal alloy composition.

1. Introduction

Copper has gained significance over other non-ferrous metals, as a base material for fabrication of electrical connectors, lead frames, and micro-electronics devices, owing to its high electrical conductivity and low cost (Jung et al., 2015). Copper is also widely used for bolts, nuts, valves, and fittings due to its excellent ductility and malleability (Nnakwo, 2017). Copper is mostly alloyed with silicon and other elements such as tungsten, zinc, tin, magnesium, manganese and nickel to gain high strength and hardness without much reduction of its conductivity (Nnakwo, 2017; Nnakwo et al., 2017a, 2017b; 2019a, 2019b; Nnakwo and Nnuka, 2018; Garbacz-Klempka et al., 2018; Qing et al., 2011; Xie et al., 2003; Lei et al., 2013a, 2013b, 2017; Gholami et al., 2017; Qian et al., 2017; Suzuki et al., 2006; Wang et al., 2016; Li et al., 2009, 2017; Pan et al., 2007; Eungyeong et al., 2011; Ho et al., 2000). Silicon increases the fluidity and hardness of copper at the expense of ductility and electrical conductivity by inducing the precipitation of hard but brittle phases such as Cu_3Si (η^I), $Cu_{15}Si_4$ (ε), and Cu_5Si (γ) when cooled slowly to ambient temperature (Pak et al., 2016; Mattern et al., 2007). Copper, when alloyed with silicon, can serve as electrode for lithium-ion battery (Polat et al., 2015; Xu et al., 2015; Moon et al., 2006) and as a catalyst for the enhancement of nanosized and nanotube zinc oxide rods production (Cai et al., 2011). Copper-silicon alloys can also be used for the fabrication of musical equipment owing to their excellent damping property (Ketut et al., 2011).

Copper acquires high strength at the expense of ductility and hardness due to precipitation of β_1-Ni_3Si + α-Cu(Ni, Si), γ'-Ni_3Al, β-Ni_3Si, and δ-Ni_2Si phases, after being doped with nickel and traces of other elements (aluminium, chromium, iron, magnesium, and tin) and subsequently aged (Qian et al., 2017; Suzuki et al., 2006; Wang et al., 2016; Pan et al., 2007; Li et al., 2009; Lei et al., 2013b; Eungyeong et al., 2011; Ho et al., 2000). Iron has been reported to cause enhancement of hardness and electrical conductivity of Cu–Si alloys containing nickel (Suzuki et al., 2006). Chromium and zirconium have been confirmed to induce microstructural refinement and precipitation of Cr_3Si and Ni_2SiZr intermetallic phases in nickel-doped Cu–Si alloys, leading to improvement of strength (Wang et al., 2016, 2018). Studies carried out by Li et al. (2017), and Wang et al. (2018) revealed that, with combined addition of

* Corresponding author.
E-mail address: kc.nnakwo@unizik.edu.ng (K.C. Nnakwo).

https://doi.org/10.1016/j.heliyon.2019.e02471
Received 7 July 2019; Received in revised form 18 August 2019; Accepted 10 September 2019
2405-8440/© 2019 The Author(s). Published by Elsevier Ltd. This is an open access article under the CC BY-NC-ND license (http://creativecommons.org/licenses/by-nc-nd/4.0/).

Table 1
Chemical composition of the developed Cu–Si–Ti alloys.

Sample	Elemental constituents (wt%)		
	Cu	Si	Ti
Cu–3Si	96.952	3	0.00
Cu–3Si-0.1Ti	96.880	3	0.12
Cu–3Si-0.3Ti	96.693	3	0.307
Cu–3Si-0.5Ti	96.471	3	0.529
Cu–3Si-0.8Ti	96.160	3	0.84
Cu–3Si–1Ti	95.714	3	1.286
Cu–3Si-1.5Ti	95.511	3	1.489

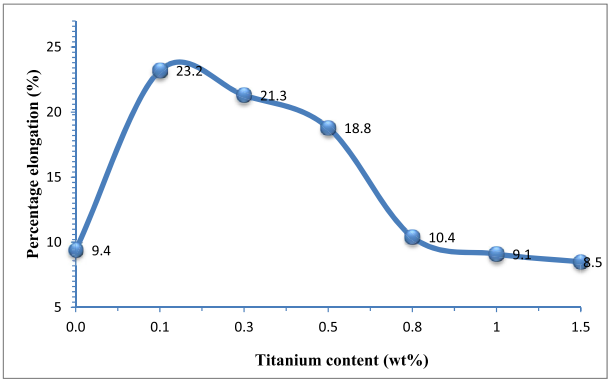

Fig. 1. Effect of titanium content on the percentage elongation of Cu–3Si-xTi alloy.

Table 2
ANOVA for conductivity and mechanical properties of the alloy compositions.

Properties	Source	Sum of sq.	*F*-value	*P*-value	*R.* sq. (%)
Percentage elongation (%)	Model	537.77	49.71	<0.0001	
	A-Ti	21.90	10.12	0.0087	95.76
	A^2	4.52	2.09	0.1762	
	A^3	7.21	3.33	0.0953	
	A^4	7.15	3.30	0.0965	
	A^5	15.07	6.97	0.0230	
Ultimate tensile strength (MPa)	Model	95484.85	529.25	<0.0001	
	A-Ti	5866.88	162.59	<0.0001	99.59
	A^2	1047.86	29.04	0.0002	
	A^3	1424.55	39.48	<0.0001	
	A^4	449.61	12.46	0.0047	
	A^5	1509.73	41.84	<0.0001	
Hardness (HV)	Model	16013.44	1561.31	<0.0001	
	A-Ti	37.53	18.29	0.0013	99.86
	A^2	24.14	11.77	0.0056	
	A^3	32.45	15.82	0.0022	
	A^4	0.1349	0.0657	0.8024	
	A^5	10.02	4.88	0.0492	
Conductivity (%IACS)	Model	6.37	20.75	<0.0001	
	A-Ti	0.8559	11.15	0.0059	87.37
	A^2	0.9675	12.61	0.0040	
	A^3	0.4960	6.46	0.0258	
	A^4	1.09	14.22	0.0027	
	A^5				
Density (g/cm^3)	Model	4.51	1044.16	<0.0001	
	A-Ti	0.0144	16.71	0.0018	
	A^2	0.0012	1.34	0.2716	99.79
	A^3	0.0219	25.39	0.0004	
	A^4	0.0033	3.78	0.0778	
	A^5	0.0149	17.21	0.0016	

chromium and zirconium to nickel-doped Cu–Si alloys, excellent hardness (122 HV-272 HV) and electrical conductivity (29.4 %IACS - 36 % IACS) are obtainable. It is pertinent to develop Cu–Si base alloys with improved ductility, hardness, and electrical conductivity, to enhance

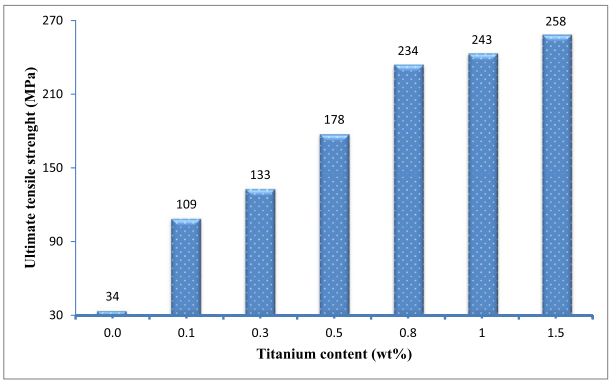

Fig. 2. Effect of titanium content on the ultimate tensile strength of Cu–3Si-xTi alloy.

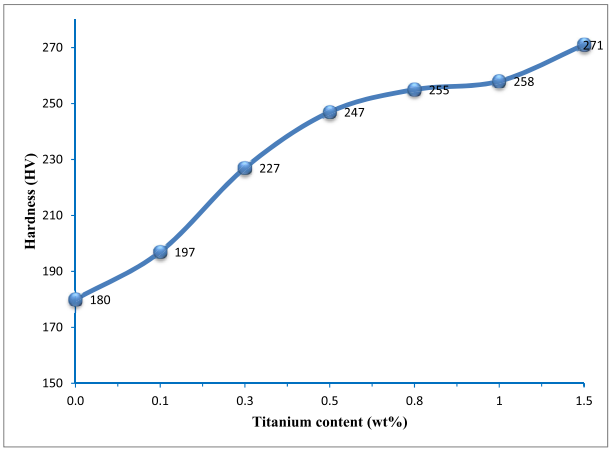

Fig. 3. Effect of titanium content on the hardness of Cu–3Si-xTi alloy.

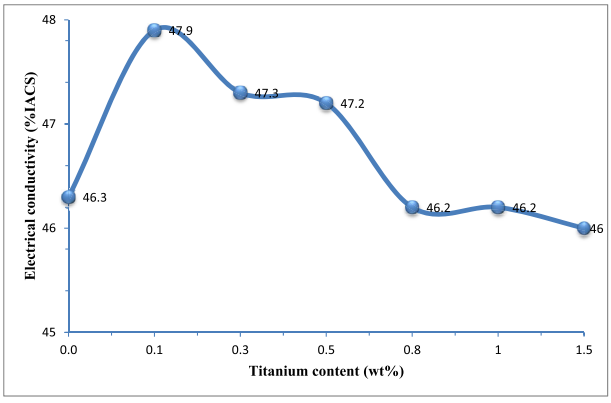

Fig. 4. Effect of titanium content on the electrical conductivity of Cu–3Si-xTi alloy.

their applications in various engineering sectors, hence this research was conducted.

This study focused on examining the influence of trace additions of titanium on grain characteristics, conductivity, and mechanical properties of copper-silicon-titanium alloys subjected to normalizing heat treatment. The impacts of average grain size and morphology on the alloy's ductility, hardness, the strength, conductivity, and density were determined. The study also examined the significance of titanium content on the tested properties using RSOD and ANOVA. The

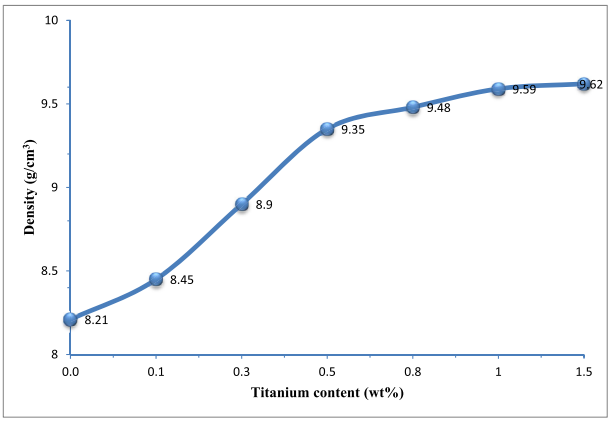

Fig. 5. Effect of titanium content on the bulk density of Cu–3Si-xTi alloy.

experimental results were optimized to obtain the optimal alloy composition and statistical model equations generated for future applications.

2. Experimental

2.1. Materials preparation

In this study, seven alloy compositions; Cu–3Si and Cu–3Si-xTi (x: 0.1, 0.3, 0.5, 0.8, 1, and 1.5 weight percent) were produced using analytical grades copper wires (99.99% pure), silicon powder (99.99% pure), and titanium powder (99.99% pure) supplied by Sigma-Aldrich. The alloys compositions were designed using RSOD; melted using a platinum crucible pot in an inert gas atmosphere. The melt was cast into a steel mold of dimension 250 mm length and 16 mm diameter and allowed to cool inside the steel mold to ambient temperature. The elemental constituents of the developed alloys were analyzed using x-ray fluorescence spectroscopy (Phillips PW2400). The developed alloys were subjected to normalizing treatment at 900 °C for 0.5 hr using a tube furnace (TSH12/25024166CG) equipped with an external thermocouple (±1 °C accuracy). The hardness test samples underwent grinding and polishing using an electric grinder and aluminium oxide powder. The tensile strength and Vickers hardness measurements were done using 100kN capacity automated

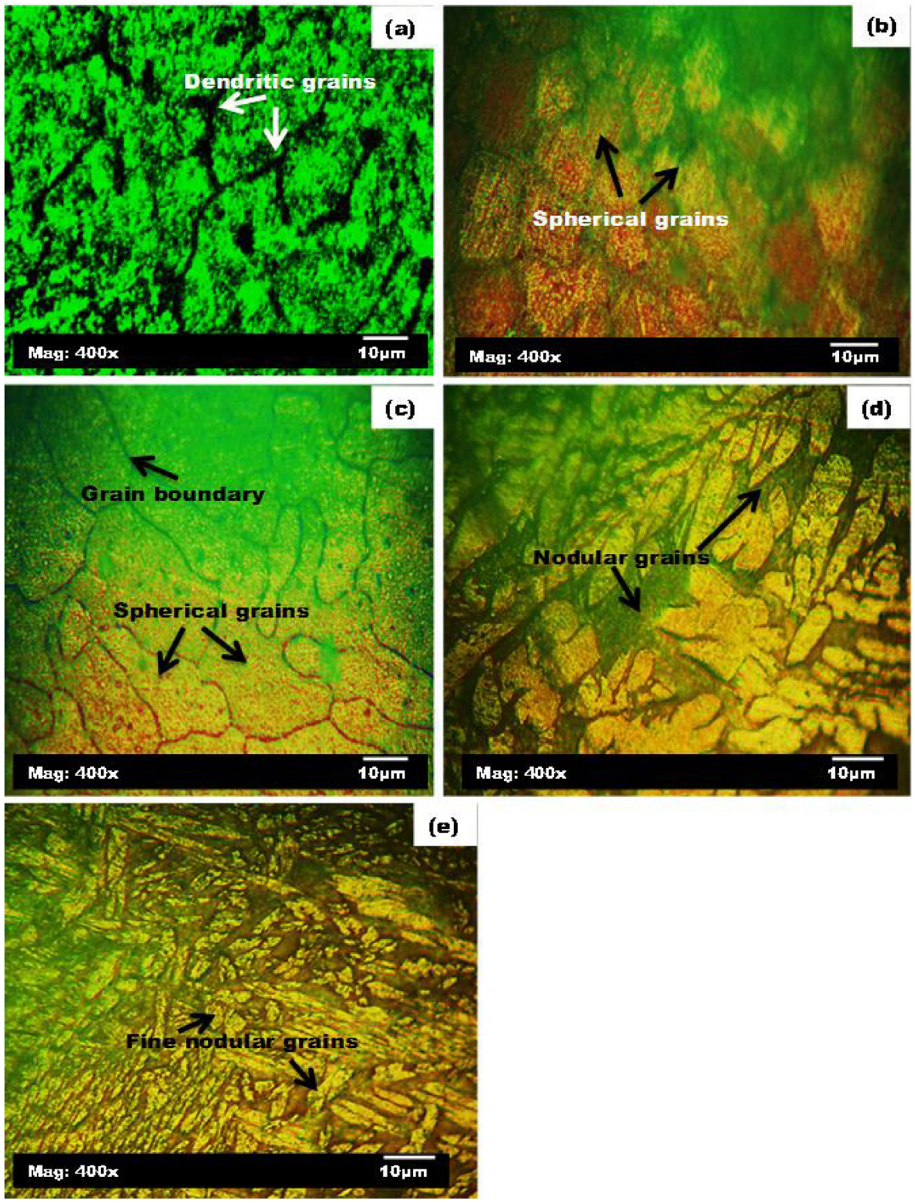

Fig. 6. Optical microstructure of (a) Cu–3Si (b) Cu–3Si-0.1Ti (c) Cu–3Si-0.5Ti (d) Cu–3Si–1Ti, and (e) Cu–3Si-1.5Ti alloys.

tensile strength tester (Model: 130812) and Vickers hardness tester (Model: VM-50) respectively. The Vickers hardness measurement was performed using a load of 183.9kgf at dwelling time of 5s. The diagonals of indentations were measured using a 20X optical microscope (Olympus BH) and the mean diameter determined. The Vickers hardness was calculated using Eq. (1). The electrical conductivity was measured using Ohms experiment as described in our previous study (Nnakwo et al., 2019b). The surface morphology of the produced alloys was examined using an optical microscope (OM, L2003A type) and Carl Zeiss SEM (EVO/NA10). The average grain size and distribution were analyzed using the linear intercept method (ImageJ software).

$$HV = 1.8544 \cdot \frac{P}{d^2} \quad (1)$$

where, HV = Vickers hardness (HV)
P = applied load (kgf)
d = average diagonals of indentations (μm)

2.2. Statistical design of experiment

Statistics are essential tools for effective designing and development of engineering materials of desirable properties at a lower cost. Researchers also utilize statistical tools for optimizing process parameters and determining the significance of factors on the quality of engineering materials (Hines et al., 2003). In this present study, the alloy compositions were designed using response surface optimal design. The experimental results were evaluated statistically using ANOVA. The experimental results were optimized to obtain the optimal alloy composition for optimal properties.

3. Results and discussion

3.1. Mechanical and physical properties of Cu–Si-xTi alloys

Table 1 outlines the results of the x-ray fluorescence spectroscopy analysis. Table 1 shows that each alloy composition contains three elements, such as copper, silicon, and titanium. The silicon content was constant in all the alloy compositions, while titanium and copper

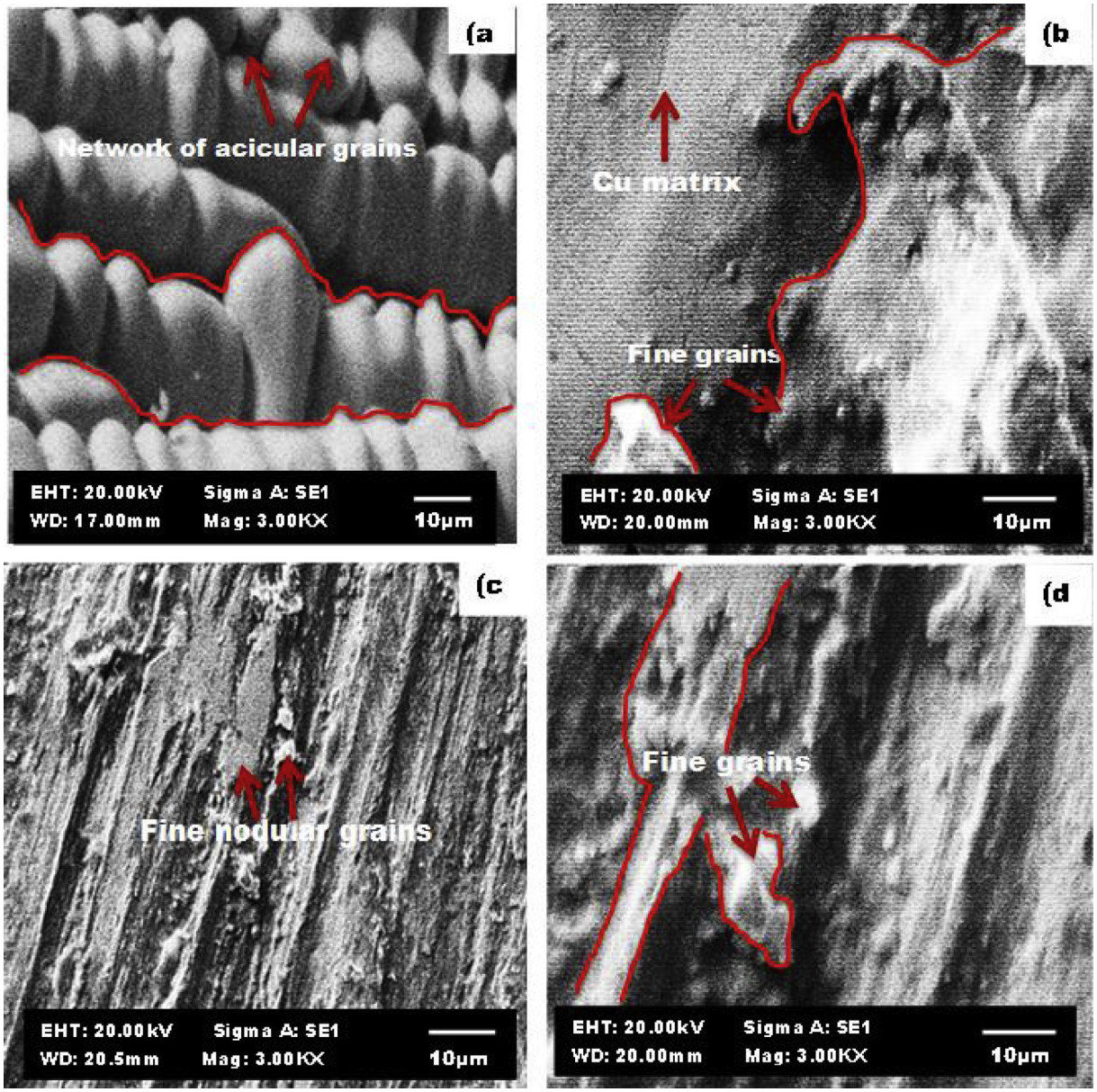

Fig. 7. Scanning electron microstructure of (a) Cu–3Si (b) Cu–3Si-0.5Ti (c) Cu–3Si–1Ti and (d) Cu–3Si-1.5Ti alloys.

contents varied. Fig. 1 shows the effect of titanium content on the percentage elongation of the parent alloy (Cu–3Si). Fig. 1 shows that the percentage elongation of the parent alloy was 9.4%. Fig. 1 shows that after adding 0.1wt% titanium to the parent alloy, its percentage elongation increased from 9.4% to 23.2%, indicating about ≈ 147% increase. The increase is significant, as demonstrated by the statistical data, having recorded *P*-value less than 0.5 (Table 2). Fig. 1 shows that the percentage elongation decreased from 23.2% to 21.3%, after increasing the titanium content in the parent alloy from 0.1 wt% to 0.3 wt%. The percentage elongation of the titanium-doped Cu–3Si alloys decreased gradually with

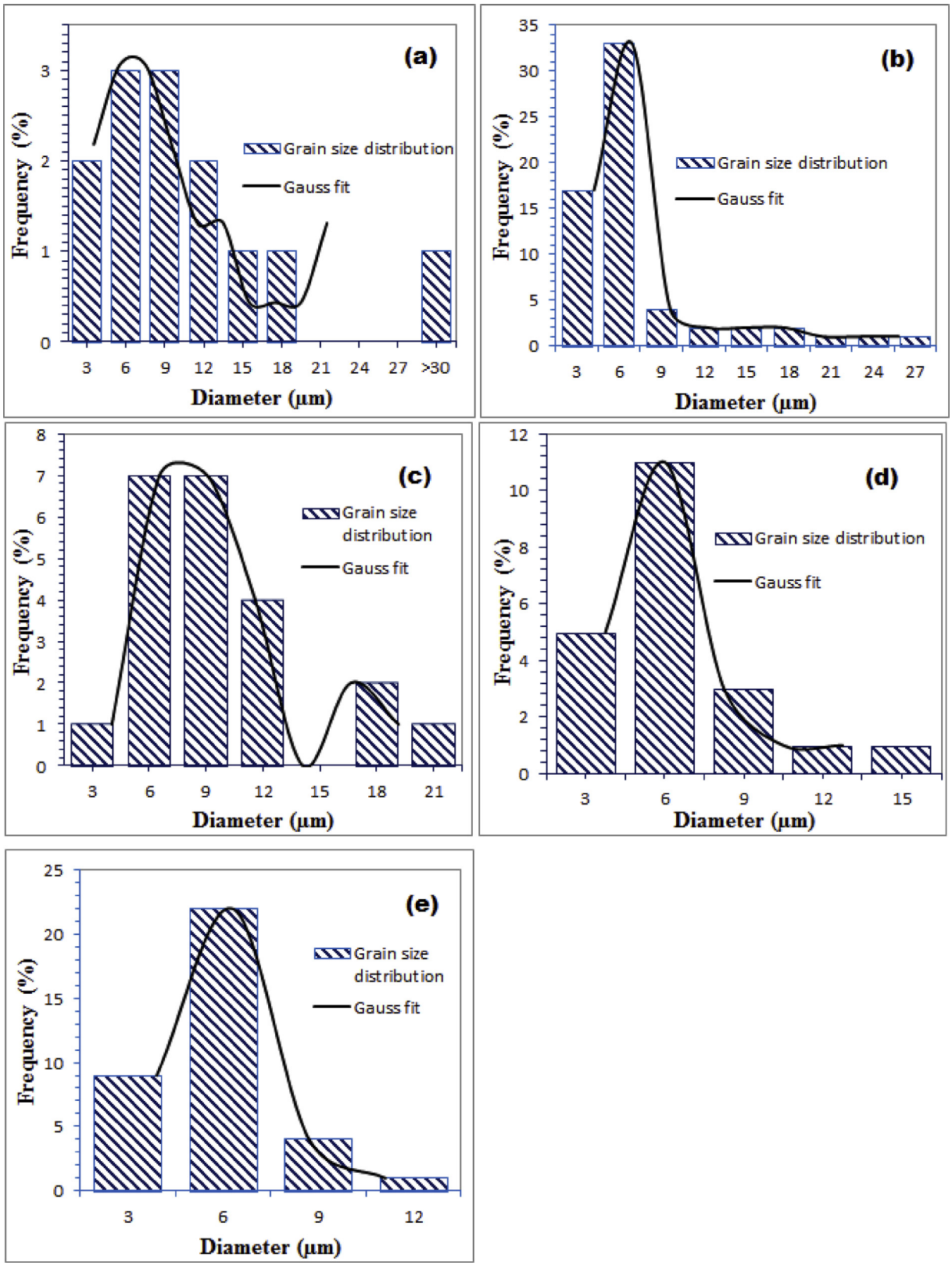

Fig. 8. Grain size distribution of (a) Cu–3Si (b) Cu–3Si-0.1Ti (c) Cu–3Si-0.5Ti (d) Cu–3Si–1Ti and (e) Cu–3Si-1.5Ti alloys.

Table 3
Optimization of experimental results and alloy compositions.

Runs	Ti content (wt%)	%E (%)	UTS (MPa)	Hardness (HV)	Conductivity (%IACS)	Density (g/cm^3)	Desirability	Remark
1	0.470	17.9	164.78	243.004	47.148	9.274	0.535	selected
2	0.990	9.0	243.14	257.624	46.221	9.578	0.368	
3	0.103	21.8	103.91	195.979	47.465	8.427	0.333	

the increasing titanium content (Fig. 1).

Fig. 2 shows the ultimate tensile strength of the parent alloy and titanium-doped Cu–3Si alloys. Fig. 2 shows that the parent alloy has the least ultimate tensile strength value. Analysis of Fig. 2 reveals that, by adding about 0.1wt% titanium to the parent alloy, the strength increased by 220.6%. The increase is statistically significant (Table 2). Fig. 2 shows that, by adding 1.5wt% titanium, the strength of the parent alloy increased by 658.82%. Fig. 3 shows the Vickers' hardness of the parent alloy and titanium-doped copper-silicon alloys. The hardness results show that the parent alloy has the least hardness value (180 HV) compared to the titanium-doped Cu–3Si alloys. The hardness value increased to 197 HV, 227 HV, 247 HV, 255 HV, 258 HV, and then to 271 HV after doping with 0.1wt%, 0.3wt%, 0.5wt%, 0.8wt%, 1wt%, and 1.5wt% titanium respectively. The increase in hardness and ultimate tensile strength can be associated with the decreasing average grain size and change in grain morphology from acicular to spherical and then to nodular pattern with increasing titanium content (Figs. 6, 7, and 8), leading to increased grain boundary area (sources of dislocation motion impediment) in the alloy structure. The strength increased systematically with the increase in the grain boundary area. Fig. 4 shows the electrical conductivity of the parent alloy and the titanium-doped Cu–Si alloys. The conductivity of the parent alloy slightly increased from 46.3 %IACS to 47.9 %IACS by adding 0.1wt% Ti. The electrical conductivity decreased slowly with increasing titanium content, resulting from the decreased average grain size. Fig. 5 shows the density of the Cu–3Si and the titanium-doped Cu–3Si alloys. The density increased gradually with increasing titanium content.

3.2. Structural examination of the developed titanium-doped Cu–3Si alloys

Figs. 6 and 7 show the optical micrograph (OM) and scanning electron microscopy (SEM) analysis of the developed alloys. Fig. 6a shows the OM of the parent alloy. Fig. 6a revealed needle-like precipitates sparsely distributed in the copper matrix. Fig. 6b–e show the OM of Cu–3Si-0.1Ti, Cu–3Si-0.5Ti, Cu–3Si–1Ti, and Cu–3Si-1.5Ti alloys. Analysis of Fig. 6b shows a change in precipitate morphology from needle-like to spherical patterns. The microstructures of Cu–3Si-0.1Ti and Cu–3Si-0.5Ti alloys have similar grain morphology, but Cu–3Si-0.5Ti alloy has more evenly dispersed grains and a greater number of grain boundaries (Fig. 6c). The microstructures of Cu–3Si–1Ti and Cu–3Si-1.5Ti alloys consist of nodular grains, with Cu–3Si-1.5Ti alloys containing more fine grains (Fig. 6d and e).

Fig. 7a shows the SEM microstructure of the parent alloy. The microstructure consists of networks of acicular grains (Fig. 7a). Fig. 7b–d show the SEM results of Cu–3Si-0.5Ti, Cu–3Si–1Ti, and Cu–3Si-1.5Ti alloys. Analysis of Fig. 7b–d shows that the microstructure of the parent alloy was effectively refined, after adding titanium, leading to increased strength and hardness. The microstructure of Cu–3Si-1.5Ti alloy consists of more fine grains, resulting in better strength and hardness as demonstrated by Figs. 2 and 3. Fig. 8 shows the grain size distribution in the developed alloys. The average grain size of the parent alloy (Cu–3Si) was ≈10.1μm, but decreased to ≈8.9 μm after adding 0.1 wt% titanium to the parent alloy, leading to improvement of mechanical properties. Fig. 8 revealed that with increasing titanium content from 0.1 wt% to 1.5 wt%, the average grain size decreased significantly from ≈8.9 μm to ≈4.4 μm resulting to about ≈659% and ≈51% increase in strength and hardness of Cu–3Si-1.5Ti alloy respectively compared to the parent alloy.

3.3. Statistical evaluation of the properties of Cu–Si–Ti alloys

Table 2 shows the results of the ANOVA for the percentage elongation, ultimate tensile strength, hardness, electrical conductivity, and density of the developed alloys. The model F-values (49.71, 529.25, 1561.31, 20.75, and 1044.16) indicated significant model terms. The *P*-values (0.0087, <0.0001, 0.0013, 0.0059, and 0.0018) were less than the limit of significance (0.05), indicating that titanium addition significantly improved the properties of the Cu–3Si alloys (Table 2). The *R*-sq. values of 95.76%, 99.59%, 99.86%, 87.37%, and 99.79% indicated the likelihood of predicting the improvements of percentage elongation, strength, hardness, electrical conductivity, and density of copper-silicon based alloys resulting from the addition of titanium.

3.3.1. Statistical model equations

Eqs. (2), (3), (4), (5), and (6) show the statistical model for predicting the percentage elongation, strength, hardness, electrical conductivity, and density of the developed alloys for a given concentration of titanium. Eqs. (2), (3), (4), (5), and (6) in terms of actual factor help in determining the relative effects of titanium content on the tested properties.

$$\%\mathbf{E} = +10.0192 + 174.2952Ti - 676.7517Ti^2 + 1004.4792Ti^3 - 667.9018Ti^4 + 164.7241Ti^5 \quad (2)$$

$$\mathbf{UTS} = +36.53 + 963.23Ti - 3679.74Ti^2 + 7057.56Ti^3 - 5784.14Ti^4 + 1648.59Ti^5 \quad (3)$$

$$\mathbf{Hardness} = +180.60 + 135.58Ti + 187.34Ti^2 - 621.99Ti^3 + 510.54Ti^4 - 134.31Ti^5 \quad (4)$$

$$\mathbf{Electrical\ conductivity} = +46.51 + 13.09Ti - 41.17Ti^2 + 40.47Ti^3 - 12.66Ti^4 \quad (5)$$

$$\mathbf{Density} = +8.222 + 1.282Ti + 8.796Ti^2 - 21.864Ti^3 + 18.319Ti^4 - 5.171Ti^5 \quad (6)$$

3.3.2. Optimization of the experimental data

Table 3 shows the optimization results of the experimental data for percentage elongation, strength, hardness, electrical conductivity, and density. Table 3 showed that Cu–3Si-0.47wt%Ti alloy was the optimal alloy composition with optimal percentage elongation (≈18%), strength (≈165 MPa), hardness (≈243 HV), conductivity (≈47 %IACS), density (≈9.3 g/cm^3) at the desirability of 0.535.

4. Conclusions

The study investigated the influence of trace additions of titanium on grain characteristics (morphology and size), conductivity, and mechanical properties of copper-silicon-titanium alloys. The OM and SEM analyses revealed that the morphology of the second phase changed in the following trends: acicular to spherical and then to nodular with increasing titanium content, resulting to increase of ductility, tensile strength, hardness, conductivity, and density by 146.8%, 658.8%, 50.6%, 3.5%, and 2.9% respectively. The increase in properties was statistically significant. The grain size of the parent alloy decreased from ≈10.1 μm to ≈8.9 μm after adding 0.1 wt% titanium leading to improvement of mechanical properties. Increasing titanium content from 0.1 wt% to 1.5 wt% led to decrease in grain size from ≈8.9 μm to ≈4.4 μm resulting to further

increase in strength and hardness. The results of optimization revealed Cu–3Si-0.47wt%Ti alloy as the optimal alloy composition with optimal percentage elongation (≈18%), strength (≈165 MPa), hardness (≈243 HV), conductivity (≈47 %IACS), density (≈9.3 g/cm^3) at the desirability of 0.535.

Declarations

Author contribution statement

Kingsley Chidi Nnakwo: Conceived and designed the experiments; Performed the experiments; Wrote the paper.

Christopher N. Mbah: Contributed reagents, materials, analysis tools or data.

Eugene E. Nnuka: Analyzed and interpreted the data.

Funding statement

This research did not receive any specific grant from funding agencies in the public, commercial, or not-for-profit sectors.

Competing interest statement

The authors declare no conflict of interest.

Additional information

No additional information is available for this paper.

Acknowledgements

The authors acknowledge the support of the management of Notex Electronics Nigeria Ltd and the management of Cutix Cable Plc, Nnewi Nigeria for providing equipment used for this research.

References

Cai, H., Tong, D., Wang, Y., Song, X., Ding, B., 2011. Reactive synthesis of porous Cu3Si compound. J. Alloy. Comp. 509, 1672–1676.

Eungyeong, L., Seungzeon, H., Kwangjun, E., Sunghwan, L., Sangshik, K., 2011. Effectof Ti addition on tensile properties of Cu-Ni-Si alloys. Met. Mater. Int. 17 (4), 569–576.

Garbacz-Klempka, A., Kozana, J., Piękoś, M., Papaj, M., Papaj, P., Perek-Nowak, M., 2018. Influence of modification in centrifugal casting on microstructure and mechanical properties of silicon bronzes. Arch. Foundry Eng. 18, 11–18.

Gholami, M., Vasely, J., Altenberger, I., Kuhn, H.A., Wollmann, M., Janecek, M., Wagner, L., 2017. Effect of microstructure on mechanical properties of CuNiSi alloys. J. Alloy. Comp. 696, 201–212.

Hines, W.W., Montgomery, D.C., Goldsman, D.M., Borror, C.M., 2003. Probability and Statistics in Engineering, fourth ed. John Wiley & Sons.

Ho, J.R., Hyung, K.B., Soon, H.H., 2000. Effect of thermo-mechanical treatments on microstructure and properties of Cu-base lead frame alloy. J. Mater. Sci. 35 (14), 3641–3646.

Jung, S.J., O'Kelly, C.J., Boland, J.J., 2015. Position controlled growth of single crystal Cu_3Si nanostructures. Cryst. Growth Des. 15, 5355–5359.

Ketut, G.S.I., Soekrisno, R., Suyitno, M.I. Made, 2011. Mechanical and damping properties of silicon bronze alloys for music applications. Int. J. Eng. Tech. IJETIJENS. 11 (06), 81–85.

Lei, Q., Li, Z., Dai, C., Wang, J., Chen, X., Xie, J.M., Yang, W.W., Chen, D.L., 2013a. Effect of aluminium on microstructure and property of Cu–Ni–Si alloys. Mater. Sci. Eng., A 572, 65–74.

Lei, Q., Li, Z., Xiao, T., Pang, Y., Xiang, Q.Z., Qiu, W.T., Xiao, Z., 2013b. A new ultrahigh strength Cu-Ni-Si alloy. Intermetallics 42, 77–84.

Lei, Q., Xiao, Z., Hu, W., Derby, B., Li, Z., 2017. Phase transformation behaviors and properties of a high strength Cu-Ni-Si alloy. Mater. Sci. Eng., A 697, 37–47.

Li, Z., Pan, Z.Y., Zhao, Y.Y., Xiao, Z., Wang, M.P., 2009. Microstructure and properties of high-conductivity, super-high-strength Cu-8.0Ni-1.8Si-0.6Sn-0.15Mg alloy. J. Mater. Res. 24 (6), 2123–2129.

Li, D., Wang, Q., Jiang, B., Li, X., Zhou, W., Dong, C., Wang, H., Chen, Q., 2017. Minor-alloyed Cu-Ni-Si alloys with high hardness and electric conductivity designed by a cluster formula approach. Prog. Nat. Sci.: Met. Mater. Int. 27 (4), 467–473.

Mattern, N., Seyrich, R., Wilde, L., Baehtz, C., Knapp, M., Acker, J., 2007. Phase formation of rapidly quenched Cu–Si alloys. J. Alloy. Comp. 429, 211–215.

Moon, T., Kim, Ch., Park, B., 2006. Electrochemical performance of amorphous-silicon thin films for lithium rechargeable batteries. J. Power Sources 155, 391–394.

Nnakwo, K.C., Okeke, I.U., Nnuka, E.E., 2017a. Structural modification and mechanical properties of Cu-3wt%Si-xwt%Sn alloy. Int. J. Sci. Res. Sci., Eng. Technol. 3, 184–187.

Nnakwo, K.C., Okeke, I.U., Nnuka, E.E., 2017b. Effect of zinc content on the structure and mechanical properties of silicon bronze. Int. J. Sci. Res. Sci., Eng. Technol. 3, 179–183.

Nnakwo, K.C., 2017. Effect of tungsten content on the structure, physical and mechanical properties of silicon bronze (Cu-3wt%Si). J. King Saud Univ. Sci.

Nnakwo, K.C., Nnuka, E.E., 2018. Correlation of the structure, mechanical and physical properties of Cu3wt%Si-xwt%Sn silicon bronze. J. Eng. Appl. Sci. 13, 83–91.

Nnakwo, K.C., Mbah, C.N., Daniel-Mkpume, C.C., 2019a. Investigation of the structural sensitive behavior of Cu-3Si-xMn ternary alloys. J. King Saud Univ. Sci. 2019.

Nnakwo, K.C., Mbah, C.N., Ude, S.N., 2019b. Influence of chemical composition on the conductivity and on some mechanical properties of Mg-doped Cu-Si alloy. J. King Saud Univ. – Eng. Sci. 2019.

Pak, A.Y., Shatrova, K.N., Aktaev, N.E., Ivashutenko, A.S., 2016. Preparation of ultrafine Cu3Si in high-current pulsed arc discharge. Nanotechnol. Russ. 11 (9– 10), 548–552.

Pan, Z.Y., Wang, M.P., Li, Z., 2007. Effect of trace elements on properties of Cu-Ni-Si alloy. Mater. Rev. 21 (5), 86–89.

Polat, B.D., Eryilmaz, O.L., Keleş, O., Erdemir, A., Amine, K., 2015. Compositionally graded SiCu thin film anode by magnetron sputtering for lithium ion battery. Thin Solid Films 596, 190–197.

Qian, L., Zhou, L., Zhou, L., Yang, G., Xi, P., Benjamin, D., 2017. Microstructure and mechanical properties of a high strength Cu-Ni-Si alloy treated by combined aging processes. J. Alloy. Comp. 695, 2413–2423.

Qing, L., Li, Z., Wang, M.P., 2011. Phase transformation behavior in Cu–8.0Ni–1.8Si alloy. J. Alloy. Comp. 509 (8), 361–367.

Suzuki, S., Shibutani, N., Mimura, K., Isshiki, M., Waseda, Y., 2006. Improvement in strength and electrical conductivity of Cu–Ni–Si alloys by aging and cold rolling. J. Alloy. Comp. 417 (1–2), 116–120.

Wang, W., Kang, H., Chen, Z., Chen, Z., Li, R., Yin, G., Wang, Y., 2016. Effects of Cr and Zr addition on microstructure and properties of Cu-Ni-Si alloys. Mater. Sci. Eng., A 673, 378–390.

Wang, W., Guo, E., Chen, Z., Kang, H., Chen, Z., Zou, C., Lia, R., Yina, G., Wang, T., 2018. Correlation between microstructures and mechanical properties of cryorolled CuNiSi alloys with Cr and Zr alloying. Mater. Char. 144, 532–546.

Xie, S.S., Li, Y.L., Zhu, L., 2003. Progress of study on lead frame copper alloy and its implementation in electronic industry. Rare Met. 27, 76–79.

Xu, K., He, Y., Ben, L., Li, H., Huang, H., 2015. Enhanced electrochemical performance of Si-Cu-Ti thin films by surface covered with Cu3Si nanowires. J. Power Sources 281, 455–460.